The *Drosophila* F Box Protein Archipelago Regulates dMyc Protein Levels In Vivo

Kenneth H. Moberg,[1,3,*] Ashim Mukherjee,[1,2]
Alexey Veraksa,[1,2] Spyros Artavanis-Tsakonas,[1]
and Iswar K. Hariharan[1,4]
[1]Massachusetts General Hospital Cancer Center
Building 149, 13th Street
Charlestown, Massachusetts 02129

Summary

Background: The Myc oncoprotein is an important regulator of cellular growth in metazoan organisms. Its levels and activity are tightly controlled in vivo by a variety of mechanisms. In normal cells, Myc protein is rapidly degraded, but the mechanism of its degradation is not well understood.

Results: Here we present genetic and biochemical evidence that Archipelago (Ago), the F box component of an SCF-ubiquitin ligase and the *Drosophila* ortholog of a human tumor suppressor, negatively regulates the levels and activity of *Drosophila* Myc (dMyc) protein in vivo. Mutations in *archipelago* (*ago*) result in strongly elevated dMyc protein levels and increased tissue growth. Genetic interactions indicate that *ago* antagonizes *dMyc* function during development. Archipelago binds dMyc and regulates its stability, and the ability of Ago to bind dMyc in vitro correlates with its ability to inhibit dMyc accumulation in vivo.

Conclusions: Our data indicate that *archipelago* is an important inhibitor of *dMyc* in developing tissues. Because *archipelago* can also regulate Cyclin E levels and Notch activity, these results indicate how a single F box protein can be responsible for the degradation of key components of multiple pathways that control growth and cell cycle progression.

Introduction

myc genes encode basic-helix-loop-helix-zipper (bHLHZ) domain transcription factors that dimerize with Max family proteins to promote cell growth and proliferation in metazoan organisms (reviewed in [1, 2]). The Myc-Max complex is implicated in the transcriptional regulation of many genes that are required for cell growth and metabolism; such genes include those for translation initiation factors and ribosomal components [2–4]. The role of Myc in promoting growth is likely to contribute to its role as an oncoprotein in a wide variety of human tumor types [5]. *myc* overexpression also promotes tumorigenesis in mice and zebrafish [6–8], indicating that

*Correspondence: kmoberg@cellbio.emory.edu
[2] These authors contributed equally to this work.
[3] Present address: Department of Cell Biology, Emory University School of Medicine, Whitehead Biomedical Research Building, 615 Michael Street, Atlanta, Georgia 30322.
[4] Present address: Department of Molecular and Cell Biology, University of California, Berkeley, 142 Life Sciences Addition #3200, Berkeley California 94720.

the oncogenic properties of *myc* genes are conserved in other organisms.

Myc deregulation in cancer occurs by a variety of mechanisms [1]. In some cancers, notably lymphomas, mutations found within the Myc protein have been shown to increase its stability [9, 10]. Myc protein is normally turned over rapidly in vivo and in cultured cells has a half-life of 20–30 min, and several studies have shown that Myc protein is subject to ubiquitin-dependent proteasomal degradation [1]. Ubiquitination of Myc in turn appears to be regulated by phosphorylation at two distinct sites in the protein's amino-terminal portion, Threonine 58 (Thr58) and Serine 62 (Ser62) [11–14]. Evidence suggests that MAP kinase mediates phosphorylation of Ser62 and that this stabilizes c-Myc. Phospho-Ser62 may be required for subsequent phosphorylation of Thr58 by glycogen-synthase kinase 3 (GSK3), which promotes the ubiquitination and degradation of c-Myc [15]. Significantly, Thr58Ile is the most common c-Myc mutation in Burkitt's lymphoma [1] and is known to stabilize Myc considerably [9, 10]. These observations suggest that phosphorylation of Thr58 by GSK3 generates a motif that facilitates the interaction of Myc with a ubiquitin ligase that restricts Myc levels and activity in vivo. Currently, the identity of the ubiquitin ligase that promotes Myc degradation has not been firmly established in any organism.

Here we implicate the *Drosophila* F box protein Archipelago (Ago) in the degradation of *Drosophila* Myc (dMyc). We find that Ago binds dMyc, and impairment of Ago function in vivo stabilizes dMyc, resulting in markedly elevated Myc levels, and promotes cell growth. Recent evidence indicates that the Fbw7/hCDC4 tumor suppressor protein, which is the human ortholog of Ago, also inhibits c-Myc accumulation by promoting its degradation [16]. Because Ago proteins also regulate Cyclin E levels [17–19] and *Notch* pathway activity (K.H.M., unpublished observations and reviewed in [20]), our findings suggest a mechanism by which the levels of Cyclin E and dMyc and the activity of the *Notch* pathway can be coordinately regulated by a shared degradation pathway.

Results

Loss of *archipelago* Accelerates Both Growth and Cell Cycle Progression

archipelago (*ago*) mutations lead to overproliferation of mutant tissue in the developing *Drosophila* eye, and we have shown that *ago* mutant cells express elevated levels of Cyclin E protein and are delayed in their exit from the cell cycle [17]. The Ago protein, as well as its human ortholog Fbw7/hCDC4, is the F box component of an SCF E3-ubiquitin ligase, and Ago binds Cyclin E and targets it for ubiquitination and subsequent degradation [17–19]. The overgrowth of *ago* mutant tissue implies that the *ago* mutant cells collectively grow (i.e., accumulate mass) at an accelerated rate in comparison
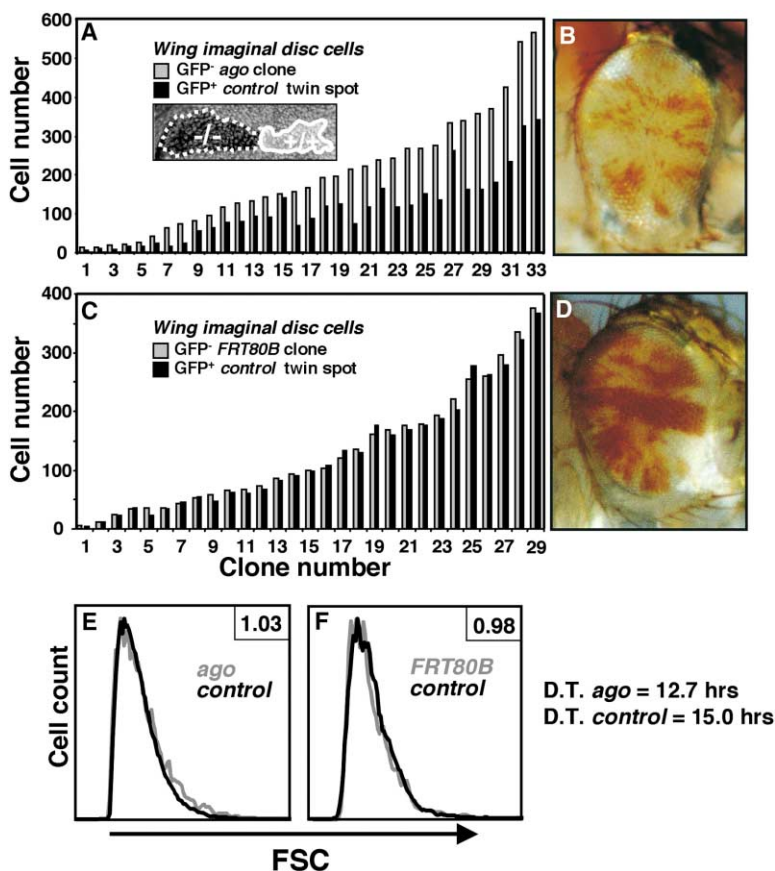
Figure 1. *ago* Mutant Cells Have a Growth Advantage

Cell numbers in wing disc clones of the (A) *ago* mutant (gray bars) or (C) *FRT80B* chromosome (gray bars), in each case compared to control twin spots (black bars). Individual clone pairs generated from the same recombination event are ordered in increasing number of mutant cells. Data from two populations of wing discs induced at time zero (a single heat shock treatment 48 hr AED) was collected 48, 72, 96, and 120 hr later and pooled. The inset in (A) shows an example of an *ago* clone/twin spot pair. Adult eyes show that (B) *ago* mutant (white) tissue overgrows compared to wild-type (red) tissue, while (D) *FRT80B* tissue does not. Forward scatter (FSC) profiles indicating that the cell size of control cells (gray line), ([E], black line) *ago* mutant cells, and ([F], black line) *FRT80B* cells are comparable. Inset values are the ratio of mean FSC values of control cells compared to *ago* cells or *FRT80B* cells. Indicated doubling times (D.T.) were calculated with data from the 72 hr time point of a single induction.

to wild-type cells (Figures 1B and 1D). Because *Drosophila* Cyclin E has been shown to promote S phase entry but not growth [21], the increased growth of *ago* mutant cells suggests that there are other Ago substrates that promote cell growth.

To examine the growth properties of *ago* mutant cells, we generated marked pairs of *ago* mutant clones and wild-type sister clones (twin spots) in the developing larval wing imaginal disc. *ago* mutant clones in the wing (Figure 1A) and the eye (Figure 1B) are consistently larger and contain more cells than their respective twin spots (labeled *control*). In contrast, pairs of clones and twin spots generated from the *FRT80B* parent chromosome do not display differences in either cell number (Figure 1C) or clone size (Figure 1D and data not shown). The increased cell number in *ago* clones indicates that *ago* mutant cells divide more frequently over a fixed period of time than do control cells and thus have a shortened cell cycle duration. Indeed, the calculated length of an average cell cycle in *ago* cells is approximately 15% shorter than in control cells (Figure 1). However, flow-cytometric analysis indicates that *ago* cells are not decreased in size (Figures 1E and 1F). These observations indicate that *ago* cells coordinately accelerate rates of cell growth and cell division such that normal cell size is maintained.

ago Cells Have Elevated dMyc Levels

To identify an SCF^{Ago} ubiquitin ligase substrate that could explain the accelerated growth of *ago* mutant

cells, we conducted two different interaction screens by using the Ago F box/WD domain (see comment in Molecular Biology section of the Experimental Procedures). By mass spectrometric analysis of proteins that coprecipitate with Ago, we identified peptides derived from a number of different SCF components, including Cullins and Skp proteins. At a lower frequency, we also recovered peptides derived from putative SCF^{Ago} substrates, including the *Drosophila* ortholog of the Myc transcription factor (dMyc). In addition to multiple SCF components, a single clone of *dMyc* was also recovered in a yeast two-hybrid screen for proteins that physically interact with the F box/WD repeat region of Ago.

Because dMyc has been shown to promote growth in imaginal-disc cells [22], the role of Ago in regulating dMyc levels was examined further. Eye imaginal discs containing *ago* mutant clones were stained with an anti-dMyc monoclonal antibody (Figures 2A–2F). dMyc protein is strongly elevated in *ago* mutant cells, both in third-larval-instar eye discs (Figures 2A–2C) and in early pupal-phase eye discs (Figures 2D–2F). Increased dMyc staining is observed in *ago* cells found throughout the larval eye disc and antennal discs. In the pupal eye disc, dMyc levels are especially high in the clusters of nuclei of the bristle cell complex (Figure 2E, arrow). Immunoblot analysis also indicates that dMyc levels are highly elevated in extracts of *ago* mutant discs compared to *FRT80B* control discs (Figure 2G). In this experiment, the twinspots carry two copies of a strong Minute mutation [*M(3)*] that dramatically impairs their growth such that
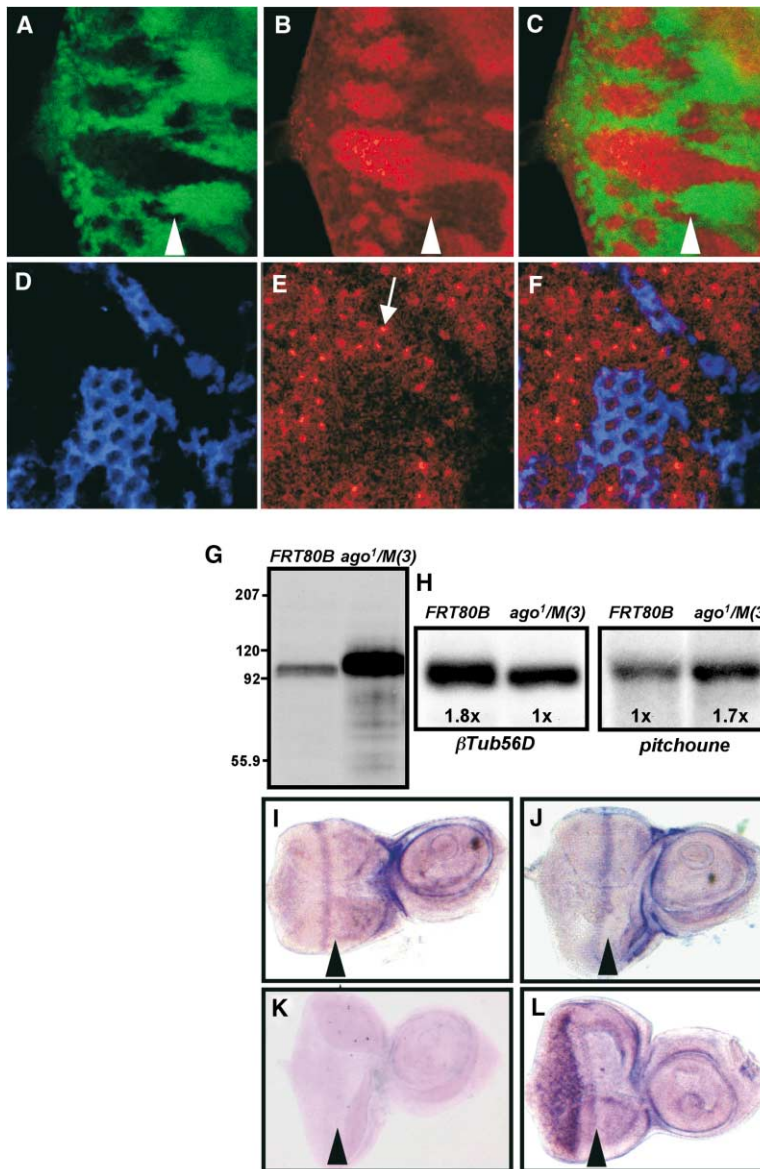
Figure 2. Loss of *ago* Deregulates dMyc Protein Levels and Results in Increased Expression of a dMyc Target Gene In Vivo

Levels of dMyc protein (red) in (A–C) third-instar and (D–F) 24 hr pupal eye discs that contain *ago* mutant clones marked by the absence of GFP (green) in (A) and (C) or by the absence of β-galactosidase (blue) in (D) and (F). Images in (C) and (F) are merges from (A) and (B) and from (D) and (E), respectively. Arrowheads in (A)–(C) denote the morphogenetic furrow. (G) Western analysis of dMyc levels in 15 pairs of *FRT80B* (left lane) or 15 pairs of *ago¹/M(3)* (right lane) third-instar larval eye discs. (H) Northern analysis of *pitchoune* and β-*Tubulin 56D* transcript levels in 4 μg of total RNA from the indicated genotypes. The difference in band intensity between adjacent lanes as determined with NIH Image is indicated. RNA in situ analysis with an anti-sense *dMyc* RNA probe shows that the levels of *dMyc* transcripts in third-instar eye discs are similar in (I) wild-type discs and in (J) *ago¹/M(3)* discs. A negative-control sense *dMyc* RNA probe produces no detectable signal in wild-type discs (K), whereas the anti-sense *dMyc* RNA probe readily detects increased *dMyc* transcripts in *pGMR-Gal4; UAS-dMyc* discs (L).

more than 95% of the disc cells are *ago* mutant (genotype denoted *ago/M(3)*). The dMyc protein detected in *ago/M(3)* discs also appears to have reduced mobility in SDS-PAGE, suggesting that in the absence of Ago, dMyc accumulates in a modified form. Significantly, overexpression of *cyclin E* in larval eye discs did not detectably alter dMyc levels (data not shown), suggesting that accumulation of dMyc protein in *ago* mutant cells is not an indirect effect of the concurrent deregulation of Cyclin E levels.

To determine if dMyc-dependent transcription is also deregulated in *ago* cells, we examined the expression of a dMyc target gene in *ago/M(3)* and *FRT80B* discs (Figure 2H). In three independent RNA preparations from equal numbers of staged discs, we observed that *ago* mutant discs contain approximately twice as much total RNA as control discs. As *ago/M(3)* and *FRT80B* discs are approximately the same size and contain similar levels of total protein (data not shown), this indicates

that *ago* mutant cells contain more RNA than control cells. The increase in the amount of RNA appears to result from a disproportionate increase in rRNA in *ago/M(3)* discs (K.H.M., unpublished observation). As a result, when equal amounts (4 μg) of total RNA are analyzed by Northern blotting, a control RNA (β-*Tubulin 56D* mRNA) is less abundant in the *ago/M(3)* sample compared to *FRT80B*. In contrast, the level of RNA of the *dMyc* target gene *pitchoune* [4, 23] is increased. If this change were normalized to the levels of β-*Tubulin 56D* RNA, this would represent an approximately 3-fold increase of *pitchoune* RNA in *ago/M(3)* discs relative to the wild-type (Figure 2H). These findings provide evidence for increased expression of a putative *dMyc* target gene in *ago* mutant cells.

To begin to examine how *ago* normally functions to inhibit dMyc levels, we performed in situ analysis of *dMyc* mRNA on *FRT80B* and *ago/M(3)* larval eye discs (Figures 2I–2L). In control discs (Figure 2I), an anti-sense

dMyc RNA probe detects *dMyc* expression at low levels throughout the eye disc, with a stronger stripe immediately posterior to the morphogenetic furrow (arrowheads), whereas a sense *dMyc* RNA probe (Figure 2K) produces no discernable staining in wild-type discs. The pattern and level of *dMyc* expression is unchanged in *ago/M(3)* discs (Figure 2J). It is possible that subtle increases in *dMyc* mRNA levels are below the limits of the detection techniques used here, but it is clear that the anti-sense *dMyc* RNA probe easily detects increased *dMyc* transcripts in *pGMR-Gal4;UAS-dMyc* eye discs (Figure 2L). These data suggest that *ago* inhibits dMyc accumulation largely through a posttranscriptional mechanism.

Ago Binds to dMyc and Regulates Its Stability

dMyc was identified as a candidate Ago binding protein, so we examined whether the ability of *ago* to regulate dMyc involves a direct interaction between Ago and dMyc (Figure 3). In protein extracts from *Drosophila* S2 cells transfected with epitope-tagged versions of Ago and dMyc (^{HA}Ago and ^{FLAG}dMyc), ^{FLAG}dMyc was readily detected in anti-HA immunoprecipitates (Figure 3A, lane 2), and in the reciprocal procedure, ^{HA}Ago was readily detected in anti-FLAG immunoprecipitates (Figure 3B, lane 2). These experiments indicate that Ago and dMyc interact physically in S2 cells. Significantly, two mutant versions of Ago, Ago[1] and Ago[3], which correspond to mutations that deregulate dMyc levels and increase growth in vivo, are dramatically impaired in their ability to interact with dMyc in cells (Figure 3C, lanes 3 and 4) despite being expressed at approximately the same level as wild-type Ago protein (Figure 3D). Thus, as is the case with the other known SCF^{Ago} substrate, Cyclin E [17], the ability of Archipelago to bind dMyc protein correlates with its ability to downregulate dMyc levels in vivo.

Coexpression of dMyc also seems to promote Ago accumulation in cells (Figure 3B, lanes 3 and 4; Figure 3C, lanes 1 and 2; Figure 4D, bottom panel, lanes 1 and 2). This increase seems more evident in forms of Ago that bind strongly to dMyc (data not shown) and does not appear to be a general effect of dMyc on all coexpressed proteins (Figure 4D, lanes 3 and 4). However, the precise mechanism underlying this effect has not been established. It may involve direct dMyc-Ago binding, but it may also be an indirect consequence of Myc's ability to regulate cell metabolism and translation rates.

Because Ago and dMyc proteins interact, we tested if perturbing Ago function in S2 cells could modulate dMyc levels and stability. A putative dominant-negative form of Ago that lacks the F box domain (AgoΔF) was constructed. AgoΔF is predicted to bind target proteins via an intact WD repeat domain but to be unable to recruit them into SCF^{Ago}. Expression of AgoΔF is thus predicted to stabilize SCF^{Ago} targets. Coexpression of dMyc and AgoΔF in cells increases the amount of Ago-dMyc complex recovered in coimmunoprecipitation experiments (Figure 3C, top panel, compare lanes 2 and 5) and increases the overall levels of dMyc in these cells (Figure 3C, bottom panel). To determine whether AgoΔF expression alters dMyc stability, we assayed dMyc lev-

els in the presence or absence of coexpressed AgoΔF protein after treatment with the translation inhibitor cycloheximide (CHX) (Figure 3E). When dMyc is expressed alone, its levels decline rapidly after CHX treatment, indicating that dMyc is normally quite unstable. In contrast, dMyc coexpressed with AgoΔF persists longer in cells after CHX addition, indicating that dMyc is more stable when SCF^{Ago} activity is reduced. In support of this, we find that treatment of cells with double-stranded *ago* RNA (dsRNA) or with the proteasome inhibitor MG132 increases the amount of transfected dMyc (Figure 3F) detected in cells. These data indicate that dMyc is degraded via the proteasome in vivo in a manner similar to mammalian c-Myc and that as the substrate specificity component of an SCF^{Ago} ubiquitin-ligase, Ago is likely to participate in this process.

A Specific Role for *archipelago* in Regulating dMyc In Vivo

In addition to Ago, one or more of the 23 other F box proteins encoded by the *Drosophila* genome [24] might also play a role in regulating dMyc levels in vivo. Of particular note are the *Drosophila* F box proteins Slmb and CG9772. The Slmb protein, encoded by the *supernumerary limbs* (*slmb*) gene [25, 26], is the *Drosophila* protein most similar to Ago within the F box and WD repeats. The gene *CG9772* may encode the *Drosophila* ortholog of the human F box protein Skp2 (54% similarity and 31% identity between CG9772-PA and Skp2 across their length), which has recently been shown to regulate c-Myc levels in a transformed mammalian cell line [27, 28].

To assess the relative roles of these F box family members in regulating endogenous dMyc levels, we used double-stranded RNA interference (dsRNAi) in S2 cells to reduce the RNA levels of *ago*, *slmb*, and *CG9772* (Figure 4A). Reducing *ago* function in S2 cells by *ago* dsRNAi results in the stabilization and accumulation of dMyc protein (Figures 4A and 4B). In contrast, despite significant reduction in the levels of *slmb* and *CG9772* RNAs, there is no discernible change in dMyc levels. We also tested whether the CG9772-PA protein (a CG9772 isoform containing the complete F box and leucine-rich repeat domains) could bind dMyc in a manner similar to Skp2, its putative human ortholog (Figures 4C and 4D). Ago and CG9772 accumulate to similar levels in the absence of coexpressed dMyc (Figure 4D, bottom panel, lanes 1 and 3). However, CG9772-PA displayed very little dMyc binding activity compared to Ago (Figures 4C and 4D, top panel). Although these data do not rule out a role for other F box proteins in regulating dMyc levels and/or activity, they do indicate that at least in S2 cells, and among the Ago, Slmb, and CG9772 proteins, only Ago is able to bind to dMyc and regulate its stability.

Genetic Interactions between *archipelago* and *dMyc*

Consistent with the observed physical interaction between the Ago and dMyc proteins, we found that an *ago* mutation could modify *dMyc* mutant phenotypes. The *dMyc* allele *diminutive¹* (*dm¹*) is a hypomorphic viable mutation caused by a gypsy element insertion into the
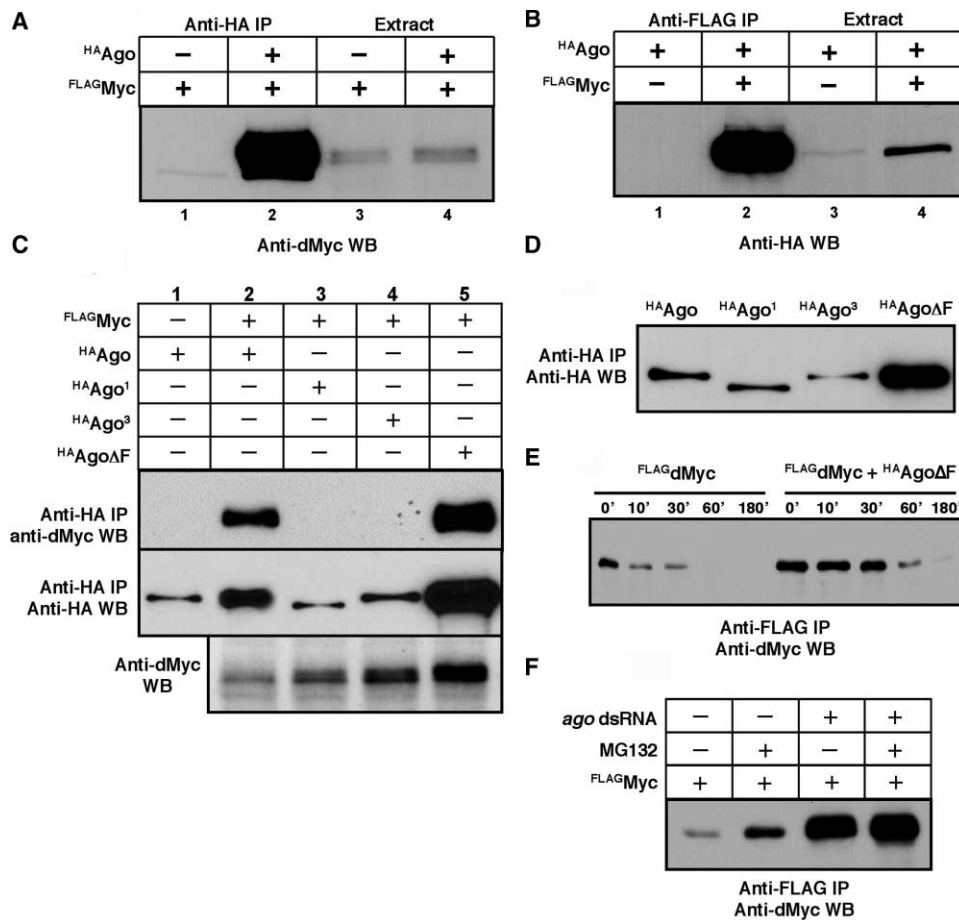
Figure 3. Archipelago Interacts with dMyc and Regulates dMyc Levels and Stability

Immunoprecipitation-immunoblot analysis of dMyc and Ago shows that dMyc is recovered with wild-type Ago ([A], lane 2) on anti-HA agarose beads and that Ago is recovered with dMyc ([B], lane 2) on anti-FLAG agarose beads from extracts of *Drosophila* S2 cells expressing HA-tagged wild-type Ago (HAAgo) and FLAG-tagged dMyc (FLAGdMyc). (C) The Ago-dMyc interaction is disrupted by *ago* mutations that lead to overgrowth in vivo (top panel, lanes 3 and 4) and is enhanced by a putative dominant-negative form of Ago that lacks the F box (top panel, lane 5) and increases the total level of dMyc protein in cells (bottom panel, lane 5). The Ago[1] protein is prematurely truncated in the WD region and migrates more quickly than full-length Ago in SDS-PAGE. (D) Mutant and wild-type forms of Ago are expressed in S2 cells at approximately equal levels. (E) dMyc levels in *Drosophila* S2 cells expressing FLAGdMyc alone (lanes 1–5) or FLAGdMyc together with the putative Archipelago dominant-negative HAAgoΔF (lanes 6–10) at the indicated time points after addition of the translation inhibitor cycloheximide (CHX). dMyc alone has a $t_{1/2}$ of less than 10 min, whereas in the presence of AgoΔF, it is stabilized with a $t_{1/2}$ of more than 30 min. (F) Levels of tagged dMyc increase in cells after treatment with either the proteasome inhibitor MG132 or double-stranded *ago* RNA to reduce Ago activity. One of two plates of *pMT-FLAG-dMyc*-expressing cells was treated with *ago* dsRNA while the other was left untreated. Each was then split in two and incubated for an additional 3 hr with or without MG132.

first intron of the *dMyc* genomic locus [29, 30]. *dm[1]* homozygous females and *dm[1]* hemizygous males are smaller than wild-type flies, and the females are sterile. *dm[1]* flies that are heterozygous for *ago* (*dm[1];ago[1]/+*) are larger than *dm[1]* flies (Figure 5A). Quantitation of this effect shows that heterozygosity for a mutation in *ago* increases *dm[1]* female body length by approximately 12% (Figure 5C). The wings of these *dm[1];ago[1]/+* adults are also approximately 15% larger than those of *dm[1]* adults (Figure 5B). To determine whether these effects are due to an increase in cell number, cell size, or both, we determined wing hair density in the relevant geno-types (Table 1). Because each cell in the wing generates a single hair, hair density varies inversely with cell size. The hair density in *dm[1]*, *dm[1];ago/+*, and wild-type wings is the same, indicating that the cells are of comparable

size. Thus, *dm[1]* wings are small because they contain fewer cells, and a 2-fold reduction in wild-type *ago* gene dosage increases the size of these mutant wings by increasing the number of normally sized cells. However, *ago* mutations do not rescue size defects associated with the *dMyc* alleles *dm[P0]* and *dm[P1]* (data not shown). These are stronger loss-of-function mutations than *dm[1]* and reduce organism size by reducing cell size, with little effect on cell number [22]. *dm[1]* may therefore represent a weaker *dMyc* allele whose body-size phenotype remains sensitive to *ago* gene dosage.

In addition to restoring cell number in the *dm[1]* mutant wings, reducing *ago* function can also ameliorate the female fertility defect of *dMyc* mutant animals (Table S1 in the Supplemental Data available with this article online). Unlike *dm[1];FRT80B/+* females, *dm[1];ago[1]/+* fe-
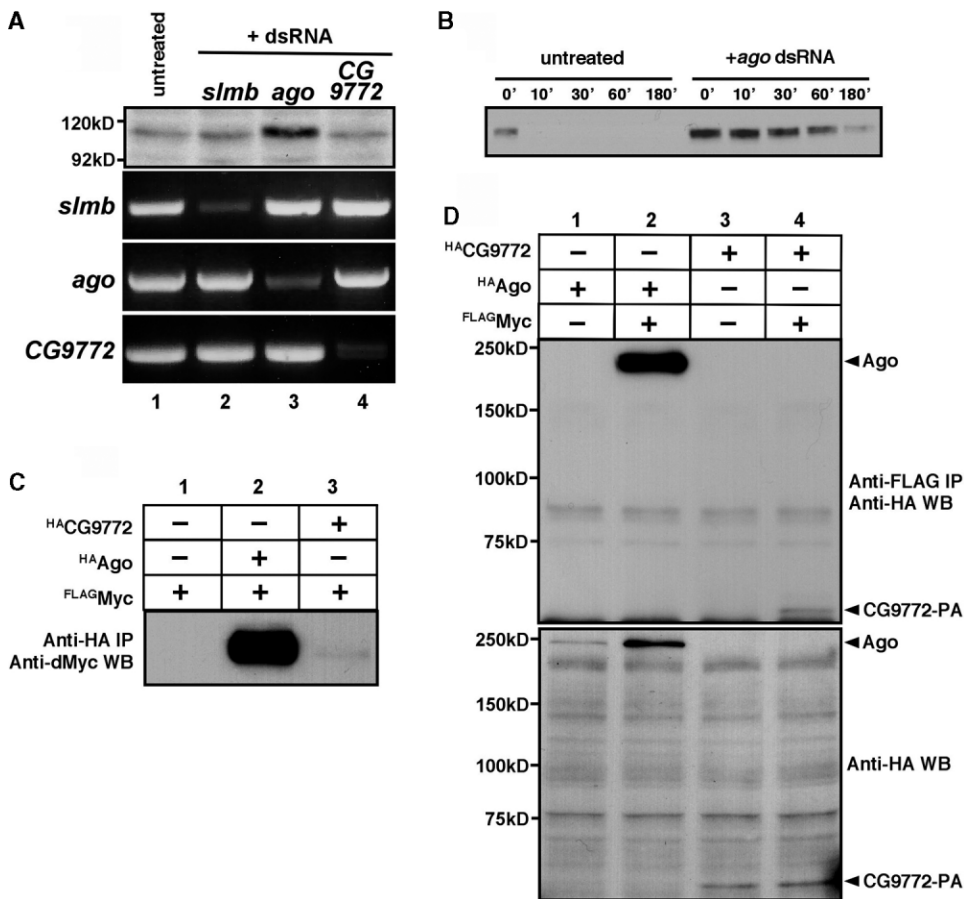
Figure 4. A Specific Role for Ago in Regulating dMyc Levels and Stability

(A) The effect of treatment with the indicated dsRNAs on dMyc protein levels (as assessed by Western blotting, top panel) or on levels of target mRNAs (as assessed by RT-PCR, bottom three panels) in *Drosophila* S2 cells. (B) Endogenous dMyc levels at the indicated time points after CHX addition in untreated S2 cells or in S2 cells treated with *ago* dsRNA. ([C and D], top panel). Side-by-side comparison of the dMyc binding properties of CG9772-PA and Ago by reciprocal immunoprecipitation-immunoblot analysis from S2 cells transfected with equal amounts of the indicated plasmids. ([D], bottom panel) Anti-HA immunoblot of S2 cell extracts expressing HA-tagged versions of Ago and CG9772-PA. The ^{HA}Ago and ^{HA}CG9772-PA bands are indicated by arrowheads.

males lay eggs that can give rise to viable larvae. In addition, $dm^1/dm^{PG45};ago/+$ females [31] are approximately 10-fold more fertile than $dm^1/dm^{PG45};FRT80B/+$ females, which normally show a 2%–3% egg hatching rate. These data indicate that, in addition to modifying *dMyc* organ and organism size phenotypes, *ago* is also an antagonist of *dMyc* in the female germline.

Consistent with a role for Ago in inhibiting dMyc, *ago* expression retards organ growth. Expression of an N-terminally truncated *ago* cDNA that contains an intact F box domain and WD repeat region in the posterior compartment of the wing decreases its size by approximately 35% (Figure 5D). Hair density measurements indicate that cells in the *ago*-expressing compartment are approximately 32% smaller than controls (Table 1), suggesting that the reduction in compartment size is largely an effect of reduced cell size. Thus, overproduction of an N-terminally truncated version of Ago in the developing wing mimics the effect of *dMyc* mutations and inhibits growth.

Discussion

We have shown that the F box-containing protein Ago, which functions as the substrate-specificity subunit of an SCF^{Ago} ubiquitin ligase, regulates the levels of the growth-promoting transcription factor dMyc in developing *Drosophila* tissues. This regulation appears to occur via a posttranscriptional mechanism that involves a direct Ago-dMyc interaction that modulates dMyc stability. dMyc accumulates in *ago* mutant cells and likely contributes to their increased growth.

**Myc and Cyclin E Share a Putative
Ago Interaction Motif**

The WD repeat domain of Ago interacts with Cyclin E [17–19], and we now show that it also binds dMyc. The optimal binding site for the WD domain of *S. cerevisiae* Cdc4, the yeast ortholog of Ago, has been determined to be I/L-I/L/P-pT-P-P, in which the central threonine residue is phosphorylated [32]. Human Cyclin E, *Dro-*
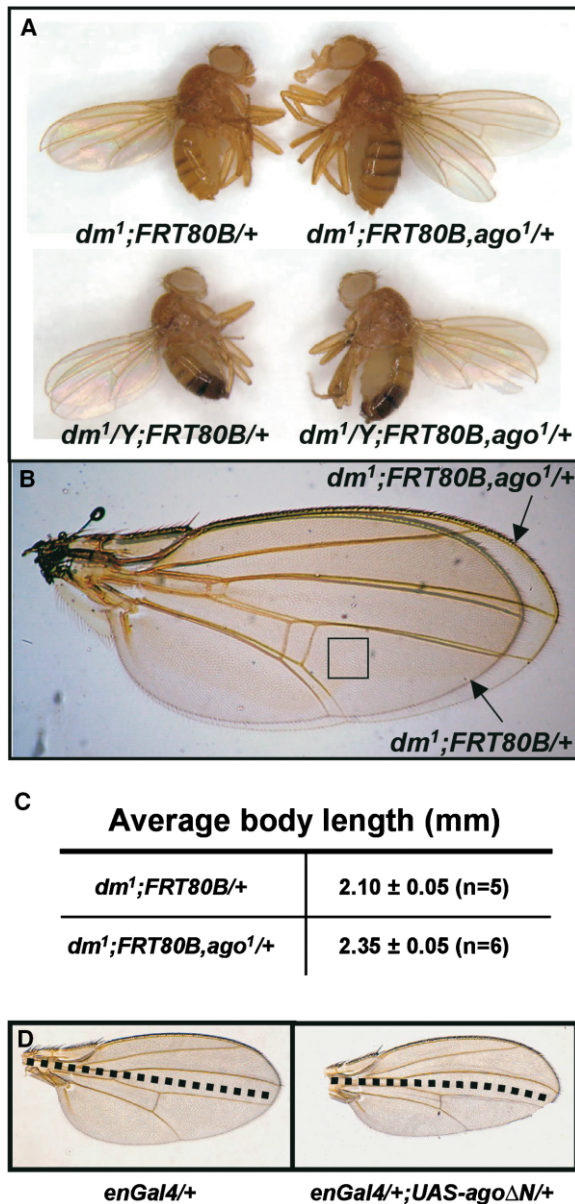

Table 1. Effect of *archipelago* on Cell Size in the Adult Wing

Genotype	Number of Hairs in Area[a]	Average Cell Area (μm^2)
wildtype (*y w*[1118])	197 ± 5.3 (n = 8)	159
y w dm¹;FRT80B/+	202 ± 6.4 (n = 8)	155
y w dm¹;FRT80B ago¹/+	197 ± 5.6 (n = 6)	159
engrailed-Gal4	199 ± 5.0 (n = 4)	158
engrailed-Gal4;UAS-ago^ΔN	291 ± 2.5 (n = 4)	108

[a] For determination of relative cell size, wings from adult female flies of the indicated genotypes were examined for trichome density. The number of trichomes was counted in a fixed area (boxed in Figure 5B) adjacent to the posterior cross vein.

which the central threonine is often replaced by a serine, and many of the flanking residues deviate from those in the consensus sequence. Importantly, these putative sites do retain a conserved S/T residue at position +4 (asterisk). The equivalent +4 serine in human Cyclin E (S384) has recently been shown to be required for the ubiquitination of Cyclin E [33] and may therefore represent an important feature of the putative Ago binding motif. The presence of multiple Ago binding sites in dMyc versus the single well-conserved site in c-Myc might indicate that although both proteins are targeted for degradation by orthologous F box proteins, the kinetics of degradation of the two Myc proteins may be different.

The array of apparently suboptimal sites in dMyc resembles the situation in *S. cerevisiae* Sic1, in which nine low-affinity sites are able to cooperatively mediate a stable interaction with Cdc4 [32, 34]. Indeed, as is the case with Sic1, mutating a single putative phosphorylation site in dMyc does not alter its Ago binding properties (Figure S1). In contrast, for human Cyclin E and c-Myc,
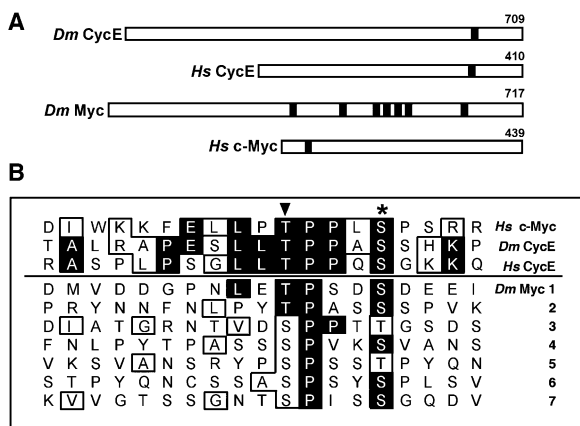
Figure 5. An *archipelago* Allele Modifies *dMyc* Organism-Size Defects, and an *archipelago* Transgene Reduces Compartment Size in the Wing

(A) An *archipelago* mutant chromosome partially suppresses the small organism size of the viable, hypomorphic *dMyc* allele *dm¹* in both females ([A], top) and males (bottom) compared to the parental *FRT80B* chromosome. (B) Overlay of adult wings shows that *dm1;ago*/+ wings are larger than *dm¹* wings. The inset square indicates the region of the wing used for cell counts in Table 1. (C) Quantitation of body-length in females of the indicated genotypes (p < 0.05). (D) Compared to control wings carrying only the *engrailed-Gal4* driver, adult wings expressing the carboxy-terminal 660 amino acids of Ago in the posterior half of the wing (*engrailed-Gal4;UAS-ago^ΔN*) display reduced posterior compartment size. A dotted line indicates the approximate border between the posterior and anterior compartments of the wing.

sophila Cyclin E, and human c-Myc all have a single, well-conserved version of this site, whose central feature is an L-L-T-P-P motif (Figure 6). dMyc contains seven copies of a degenerate version of this site, in

Figure 6. Myc and Cyclin E Share a Putative Ago Interaction Motif

(A) The location of candidate Ago interaction motifs (black boxes) in human Cyclin E, human c-Myc, *Drosophila* Cyclin E, and *Drosophila* Myc.

(B) Amino acid comparison between these motifs suggests that a single high-affinity phospho-epitope is conserved in human Cyclin E, human c-Myc, and fly Cyclin E and that multiple phospho-epitope sites may be present in dMyc. Identical (black boxes) and similar (open boxes) residues are indicated. The central S/T residue is marked by an arrowhead, and the conserved S/T residue at position +4 is marked by an asterisk.

the predicted Ago interaction site lies within a domain previously shown to be required for their ubiquitination and degradation [9, 10, 35, 36]. Furthermore, missense mutations of the central threonine in the Ago interaction motif are the most frequent c-Myc mutations in Burkitt's lymphoma [1] and stabilize c-Myc in cells [9, 10], suggesting that Ago-dependent degradation of c-Myc is perturbed in these cancers.

Regulation of Growth and Cell Proliferation by *ago*

ago mutant cells grow more quickly than their wild-type neighbors, but they maintain their normal size by an apparent acceleration of the cell cycle. This differs considerably from the phenotype elicited by overexpression of either dMyc or Cyclin E. Increased expression of dMyc results in increased growth that manifests as an increase in cell size without any change in the duration of the cell cycle [22]. dMyc also promotes S phase entry, possibly as a consequence of the increased growth. Increased expression of Cyclin E has no effect on growth but promotes S phase entry [21]. It also results in, at best, a modest acceleration of the cell cycle. Thus, the cell cycle acceleration observed in *ago* mutant cells is not easily explained by the elevated level of either dMyc or Cyclin E. Both dMyc and Cyclin E promote S phase entry but maintain the normal duration of the cell cycle by apparently lengthening the S and G2 phases, respectively. Thus, it seems likely that *ago* loss also affects a regulatory protein that promotes the G_2-M transition. Such a regulator could either be a direct substrate of SCF^{Ago} or may be regulated indirectly.

Interestingly, both Ago targets identified to date, Cyclin E and dMyc, are required for imaginal-disc growth. We have also observed that signaling via the Notch receptor is increased in *ago* clones (data not shown), as assessed by the activity of a reporter gene fused to the *Enhancer of split* mβ promoter [37]. *Notch* signaling has been shown to promote imaginal-disc growth at least in part by a non-cell-autonomous pathway [38]. Because *cyclin E*, *dMyc*, and *Notch* all participate in tissue growth via increases in cell number and/or cell mass, Ago may represent a way to coordinately regulate these pathways by a common degradation mechanism. Thus, increased Ago levels would be expected to impair tissue growth, and decreased levels would facilitate tissue growth, via multiple pathways. Because we have previously shown that *ago* transcription is patterned in the eye imaginal disc [17], *ago* may function to link patterning signals with the activity of these growth-promoting pathways.

The ability of *ago* to regulate multiple pathways that function in growing cells has implications for understanding the role of its human ortholog (Fbw7/hCDC4) as a tumor suppressor gene. We and others have identified mutations in Fbw7/hCDC4 in cancer cell lines [17, 18], and more recently, mutations have been identified in Fbw7/hCDC4 in endometrial and colorectal tumors [39, 40]. These tumors are likely to have elevated levels of Cyclin E. In light of the data presented here, they are predicted to have high levels of the oncoprotein c-Myc and increased *Notch* activity, which has also been implicated in human cancers [41]. Thus, the neoplastic phe-notype of these tumors may reflect the additive effect of activating all of these pathways that are normally inhibited by Ago.

Experimental Procedures

Drosophila Genetics

Unless indicated, flies were maintained at 25°C. To generate "*ago/ M(3)*" discs, the 3L *Minute P[mini-w]Rpl14¹* (Bloomington Stock Center) was recombined onto the *FRT80B* chromosome, and *y w eyFLP; FRT80B P[mini-w]Rpl14¹/TM6B* virgin females were crossed to *w;FRT80B ago¹* males to generate *y w eyFLP/+;FRT80B ago¹/ FRT80B P[mini-w]Rpl14¹* animals with "*ago/M(3)*" eye discs. Other genotypes used were as follows: *w;FRT80B ago¹/TM6B, y w eyFLP; FRT80B P[mini-w;arm-lacZ], y w eyFLP;FRT80B P[mini-w] P[Ubi-GFP]/TM6B, y w hsFLP;FRT80B P[mini-w] P[Ubi-GFP]/TM6B, dm¹/ FM7c; FRT80B ago¹/TM6B, dm¹/FM7c; FRT80B/TM6B*, and *dm^{PG45}/ FM7c. dMyc* stocks were a gift of R. Eisenman.

Molecular Biology

Drosophila Myc copurified with TAP(tandem affinity purification)-tagged Ago expressed in *Drosophila* Kc cells [42, 43]. Cell extraction, purification, and mass-spectrometric identification of copurifying proteins (Taplin Mass Spectrometry Facility, Harvard Medical School) were performed via procedures modified for *Drosophila* cells [44]. *dMyc* was also recovered in a standard two-hybrid screen in which approximately 5.0×10^6 colonies of a random-primed *Drosophila* 0–24 hr embryonic cDNA library were sceened with a cDNA corresponding to amino acids 681–1325 of *Drosophila* Ago fused in-frame to the LexA DNA binding domain [45].

For expression in cells, full-length *archipelago, CG9772-PA*, and *dMyc* open reading frames were amino-terminally tagged with either HA (*ago* and *CG9772-PA*) or Flag (*dMyc*) tags and cloned into *pMT* expression vectors (Invitrogen). ^{HA}Ago¹ and ^{HA}Ago³ carry point mutations corresponding to *ago* alleles described previously [17]. *pMT-HA-agoΔF* was constructed from *pMT-HA-ago* with the QuikChange Kit (Stratagene) for removal of codons 895–923, representing the core Ago F box. *UAS-agoΔN* was constructed by insertion of the C-terminal 660 codons of the *archipelago* cDNA (designated *agoΔN*) into the EcoR1 site of the *pUAST* vector.

Cell Culture and Transfection

Drosophila S2 cells were maintained at 25°C in standard Schneider cell medium (JRH Biosciences) supplemented with 10% fetal calf serum. Equal numbers of cells were transfected as indicated with 3 μg of each expression vector per 10 cm plate via the Effectene reagent (Qiagen). Transfections were done in parallel, and DNA amounts were normalized with empty vector. The *pIE14-GFP* expression vector (Novagen) was used in some experiments (0.1 μg) to monitor transfection efficiency. CuSO₄ (0.35 mM) was added to cells 24 hr after transfection to induce protein expression for 12 hr prior to analysis. Transfection of dsRNA-treated cells was performed as described above 3 days after the addition of dsRNA (see below), with the addition of 3 μg of dsRNA to the transfection mix. After CuSO₄ addition, cells were treated where indicated with the proteasome inhibitor MG132 (50 μM; Calbiochem) for 3 hr prior to analysis.

RNA Interference, In Situ, and Northern Analysis

Double-stranded RNA interference treatments were carried out as described in [46], and cells were harvested for analysis 5 days later. The RiboMax-T7 system (Promega) was used to prepare dsRNAs from PCR products generated from primer pairs specific to *ago*, *CG9772*, and *slmb* (see Supplemental Data). Analysis of *ago*, *slmb*, and *CG9772* mRNA levels in dsRNA-treated cells was carried out with the Titanium One-Step RT-PCR Kit (BD Biosciences). RNA for Northern blotting was prepared with the Trizol Reagent (Gibco-BRL). Blots were hybridized with *pitchoune* or β-*Tubulin 56D* ³²P-labeled DNA probes in ULTRAhyb hybridization buffer (Ambion). For RNA in situ analysis, the sense and anti-sense *dMyc* RNA probes were derived from the full-length *dMyc* open-reading frame.

Immunoprecipitation and Western Blotting
Cell extracts were prepared in a lysis buffer containing 0.4% NP-40 and protease inhibitors. Equal amounts of extracted proteins were then incubated for 1–2 hr with anti-HA or anti-Flag agarose (Sigma) and washed three times with lysis buffer, and the samples were resolved by 7.5% SDS-PAGE prior to Western blotting (WB) with anti-HA or anti-FLAG antibodies (1:5000; Sigma) or anti-dMyc antibody (1:20; mouse monoclonal P4C4-b10).

Microscopy, Immunohistochemistry, and Flow Cytometry
Adult eyes were photographed while submerged in mineral oil. Whole-mount flies and wings were prepared and photographed via standard techniques. For immunofluorescence, discs were fixed and stained as described previously [17]. The P4C4-b10 antibody was used undiluted. Anti-β-galactosidase rabbit polyclonal antibody (Cappel), anti-rabbit Cy5, and anti-mouse Cy3 (Jackson Laboratories) were used at 1:100. FACS and loss-of-function wing clone analysis were performed as described previously [47]. In brief, clones were induced by a 30 min heat-shock at 37°C 48 hr after egg deposition (AED), and wing discs were dissected for analysis 48, 72, 96, and 120 hr later. The genotypes were *y w hsFLP/+;FRT80B/FRT80B Pmini-w] P[Ubi-GFP]* and *y w hsFLP/+; FRT80B ago¹/FRT80B Pmini-w] P[Ubi-GFP]*. The doubling-times of the *ago*, *FRT80B* and GFP+ tester (*control*) chromosomes were calculated as described previously [22] with cell-count data collected 72 hr after induction. The *FRT80B* and *control* chromosomes gave similar results (data not shown).

Supplemental Data
Supplemental data including a table and two figures are available with this article online at http://www.current-biology.com/cgi/content/full/14/11/965/DC1/.

References

1. Grandori, C., Cowley, S.M., James, L.P., and Eisenman, R.N. (2000). The Myc/Max/Mad network and the transcriptional control of cell behavior. Annu. Rev. Cell Dev. Biol. *16*, 653–699.
2. Levens, D.L. (2003). Reconstructing MYC. Genes Dev. *17*, 1071–1077.
3. Fernandez, P.C., Frank, S.R., Wang, L., Schroeder, M., Liu, S., Greene, J., Cocito, A., and Amati, B. (2003). Genomic targets of the human c-Myc protein. Genes Dev. *17*, 1115–1129.
4. Orian, A., Van Steensel, B., Delrow, J., Bussemaker, H.J., Li, L., Sawado, T., Williams, E., Loo, L.W., Cowley, S.M., Yost, C., et al. (2003). Genomic binding by the Drosophila Myc, Max, Mad/Mnt transcription factor network. Genes Dev. *17*, 1101–1114.
5. DePinho, R.A., Schreiber-Agus, N., and Alt, F.W. (1991). myc family oncogenes in the development of normal and neoplastic cells. Adv. Cancer Res. *57*, 1–46.
6. Adams, J.M., Harris, A.W., Pinkert, C.A., Corcoran, L.M., Alexander, W.S., Cory, S., Palmiter, R.D., and Brinster, R.L. (1985). The c-myc oncogene driven by immunoglobulin enhancers induces lymphoid malignancy in transgenic mice. Nature *318*, 533–538.
7. Langenau, D.M., Traver, D., Ferrando, A.A., Kutok, J.L., Aster, J.C., Kanki, J.P., Lin, S., Prochownik, E., Trede, N.S., Zon, L.I., et al. (2003). Myc-induced T cell leukemia in transgenic zebrafish. Science *299*, 887–890.
8. Stewart, T.A., Pattengale, P.K., and Leder, P. (1984). Spontaneous adenocarcinomas in transgenic mice that carry and express MTV/myc fusion genes. Cell *38*, 627–637.
9. Salghetti, S.E., Kim, S.Y., and Tansey, W.P. (1999). Destruction of Myc by ubiquitin-mediated proteolysis: cancer-associated and transforming mutations stabilize Myc. EMBO J. *18*, 717–726.
10. Gregory, M.A., and Hann, S.R. (2000). c-Myc proteolysis by the ubiquitin-proteasome pathway: stabilization of c-Myc in Burkitt's lymphoma cells. Mol. Cell. Biol. *20*, 2423–2435.
11. Henriksson, M., Bakardjiev, A., Klein, G., and Luscher, B. (1993). Phosphorylation sites mapping in the N-terminal domain of c-myc modulate its transforming potential. Oncogene *8*, 3199–3209.
12. Lutterbach, B., and Hann, S.R. (1994). Hierarchical phosphorylation at N-terminal transformation-sensitive sites in c-Myc protein is regulated by mitogens and in mitosis. Mol. Cell. Biol. *14*, 5510–5522.
13. Pulverer, B.J., Fisher, C., Vousden, K., Littlewood, T., Evan, G., and Woodgett, J.R. (1994). Site-specific modulation of c-Myc cotransformation by residues phosphorylated in vivo. Oncogene *9*, 59–70.
14. Sears, R., Nuckolls, F., Haura, E., Taya, Y., Tamai, K., and Nevins, J.R. (2000). Multiple Ras-dependent phosphorylation pathways regulate Myc protein stability. Genes Dev. *14*, 2501–2514.
15. Gregory, M.A., Qi, Y., and Hann, S.R. (2003). Phosphorylation by glycogen synthase kinase-3 controls c-myc proteolysis and subnuclear localization. J. Biol. Chem. *278*, 51606–51612.
16. Welcker. M. Orian, A. Jin, J., Harper, J.W., Eisenman, R.N., and Clurman, B.E. (2004). The Fbw7 tumor supressor regulates GSK3 phosphorylation-dependent c-Myc protein degradation. Proc. Natl. Acad. Sci. USA, in press.
17. Moberg, K.H., Bell, D.W., Wahrer, D.C., Haber, D.A., and Harihan, I.K. (2001). Archipelago regulates Cyclin E levels in Drosophila and is mutated in human cancer cell lines. Nature *413*, 311–316.
18. Strohmaier, H., Spruck, C.H., Kaiser, P., Won, K.A., Sangfelt, O., and Reed, S.I. (2001). Human F-box protein hCdc4 targets cyclin E for proteolysis and is mutated in a breast cancer cell line. Nature *413*, 316–322.
19. Koepp, D.M., Schaefer, L.K., Ye, X., Keyomarsi, K., Chu, C., Harper, J.W., and Elledge, S.J. (2001). Phosphorylation-dependent ubiquitination of cyclin E by the SCFFbw7 ubiquitin ligase. Science *294*, 173–177.
20. Justice, N.J., and Jan, Y.N. (2002). Variations on the Notch pathway in neural development. Curr. Opin. Neurobiol. *12*, 64–70.
21. Neufeld, T.P., de la Cruz, A.F., Johnston, L.A., and Edgar, B.A. (1998). Coordination of growth and cell division in the Drosophila wing. Cell *93*, 1183–1193.
22. Johnston, L.A., Prober, D.A., Edgar, B.A., Eisenman, R.N., and Gallant, P. (1999). Drosophila myc regulates cellular growth during development. Cell *98*, 779–790.
23. Zaffran, S., Chartier, A., Gallant, P., Astier, M., Arquier, N., Doherty, D., Gratecos, D., and Semeriva, M. (1998). A Drosophila RNA helicase gene, pitchoune, is required for cell growth and proliferation and is a potential target of d-Myc. Development *125*, 3571–3584.
24. Das, T., Purkayastha-Mukherjee, C., D'Angelo, J., and Weir, M. (2002). A conserved F-box gene with unusual transcript localization. Dev. Genes Evol. *212*, 134–140.
25. Jiang, J., and Struhl, G. (1998). Regulation of the Hedgehog and Wingless signalling pathways by the F-box/WD40-repeat protein Slimb. Nature *391*, 493–496.
26. Theodosiou, N.A., Zhang, S., Wang, W.Y., and Xu, T. (1998). slimb coordinates wg and dpp expression in the dorsal-ventral and anterior-posterior axes during limb development. Development *125*, 3411–3416.
27. Kim, S.Y., Herbst, A., Tworkowski, K.A., Salghetti, S.E., and

Tansey, W.P. (2003). Skp2 regulates myc protein stability and activity. Mol. Cell *11*, 1177–1188.

28. von der Lehr, N., Johansson, S., Wu, S., Bahram, F., Castell, A., Cetinkaya, C., Hydbring, P., Weidung, I., Nakayama, K., Nakayama, K.I., et al. (2003). The F-box protein Skp2 participates in c-Myc proteosomal degradation and acts as a cofactor for c-Myc-regulated transcription. Mol. Cell *11*, 1189–1200.

29. Gallant, P., Shiio, Y., Cheng, P.F., Parkhurst, S.M., and Eisenman, R.N. (1996). Myc and Max homologs in Drosophila. Science *274*, 1523–1527.

30. Schreiber-Agus, N., Stein, D., Chen, K., Goltz, J.S., Stevens, L., and DePinho, R.A. (1997). Drosophila Myc is oncogenic in mammalian cells and plays a role in the diminutive phenotype. Proc. Natl. Acad. Sci. USA *94*, 1235–1240.

31. Bourbon, H.M., Gonzy-Treboul, G., Peronnet, F., Alin, M.F., Ardourel, C., Benassayag, C., Cribbs, D., Deutsch, J., Ferrer, P., Haenlin, M., et al. (2002). A P-insertion screen identifying novel X-linked essential genes in Drosophila. Mech. Dev. *110*, 71–83.

32. Nash, P., Tang, X., Orlicky, S., Chen, Q., Gertler, F.B., Mendenhall, M.D., Sicheri, F., Pawson, T., and Tyers, M. (2001). Multisite phosphorylation of a CDK inhibitor sets a threshold for the onset of DNA replication. Nature *414*, 514–521.

33. Welcker, M., Singer, J., Loeb, K.R., Grim, J., Bloecher, A., Gurien-West, M., Clurman, B.E., and Roberts, J.M. (2003). Multisite phosphorylation by Cdk2 and GSK3 controls Cyclin E degradation. Mol. Cell *12*, 381–392.

34. Orlicky, S., Tang, X., Willems, A., Tyers, M., and Sicheri, F. (2003). Structural basis for phosphodependent substrate selection and orientation by the SCFCdc4 ubiquitin ligase. Cell *112*, 243–256.

35. Won, K.A., and Reed, S.I. (1996). Activation of cyclin E/CDK2 is coupled to site-specific autophosphorylation and ubiquitin-dependent degradation of cyclin E. EMBO J. *15*, 4182–4193.

36. Clurman, B.E., Sheaff, R.J., Thress, K., Groudine, M., and Roberts, J.M. (1996). Turnover of cyclin E by the ubiquitin-proteasome pathway is regulated by cdk2 binding and cyclin phosphorylation. Genes Dev. *10*, 1979–1990.

37. de Celis, J.F., Tyler, D.M., de Celis, J., and Bray, S.J. (1998). Notch signalling mediates segmentation of the Drosophila leg. Development *125*, 4617–4626.

38. Go, M.J., Eastman, D.S., and Artavanis-Tsakonas, S. (1998). Cell proliferation control by Notch signaling in Drosophila development. Development *125*, 2031–2040.

39. Spruck, C.H., Strohmaier, H., Sangfelt, O., Muller, H.M., Hubalek, M., Muller-Holzner, E., Marth, C., Widschwendter, M., and Reed, S.I. (2002). hCDC4 gene mutations in endometrial cancer. Cancer Res. *62*, 4535–4539.

40. Rajagopalan, H., Jallepalli, P.V., Rago, C., Velculescu, V.E., Kinzler, K.W., Vogelstein, B., and Lengauer, C. (2004). Inactivation of hCDC4 can cause chromosomal instability. Nature *428*, 77–81.

41. Maillard, I., and Pear, W.S. (2003). Notch and cancer: best to avoid the ups and downs. Cancer Cell *3*, 203–205.

42. Rigaut, G., Shevchenko, A., Rutz, B., Wilm, M., Mann, M., and Seraphin, B. (1999). A generic protein purification method for protein complex characterization and proteome exploration. Nat. Biotechnol. *17*, 1030–1032.

43. Gavin, A.C., Bosche, M., Krause, R., Grandi, P., Marzioch, M., Bauer, A., Schultz, J., Rick, J.M., Michon, A.M., Cruciat, C.M., et al. (2002). Functional organization of the yeast proteome by systematic analysis of protein complexes. Nature *415*, 141–147.

44. Puig, O., Caspary, F., Rigaut, G., Rutz, B., Bouveret, E., Bragado-Nilsson, E., Wilm, M., and Seraphin, B. (2001). The tandem affinity purification (TAP) method: a general procedure of protein complex purification. Methods *24*, 218–229.

45. Fromont-Racine, M., Rain, J.C., and Legrain, P. (2002). Building protein-protein networks by two-hybrid mating strategy. Methods Enzymol. *350*, 513–524.

46. Worby, C.A., Simonson-Leff, N., and Dixon, J.E. (2001). RNA interference of gene expression (RNAi) in cultured Drosophila cells. Sci STKE *2001*, PL1.

47. Tapon, N., Ito, N., Dickson, B.J., Treisman, J.E., and Hariharan, I.K. (2001). The Drosophila tuberous sclerosis complex gene homologs restrict cell growth and cell proliferation. Cell *105*, 345–355.

Note Added in Proof

While this manuscript was in review, work from the group of K.I. Nakayama describing a similar role for murine Fbw7 in the degradation of c-Myc was published online in the EMBO journal.